Organic Process Research & Development

Article

pubs.acs.org/OPRD

Versatile Microfluidic Approach to Crystallization

S. Zhang, N. Ferté, N. Candoni, and S. Veesler*

CNRS, CINaM, Aix-Marseille Université Campus de Luminy, Case 913, 13288 Marseille Cedex 09, France

Supporting Information

ABSTRACT: We present a simple and easy-to-use microfluidic setup for the crystallization of mineral, organic, and biological materials. After briefly presenting the hydrodynamic properties of the setup, we test and validate it with viscous media by crystallizing a protein in an aqueous solution of PEG. We obtain nucleation data in nanocrystallizers using a droplet-based method and precisely controlling input flows to test different crystallization conditions.

INTRODUCTION

A better understanding and control of crystallization will open the way to new approaches to crystallization in production, for instance of pharmaceuticals and nanomaterials. Crystallization is influenced by several parameters such as supersaturation, temperature, chemical composition, and hydrodynamics. Rapid screening of phases and crystallization conditions is, therefore, often required during the study of the crystallization of a material. High-Throughput Screening (HTS), initially developed for biocrystallization[1] and applied in the pharmaceutical industry,[2] is used for this purpose. But sometimes only a small quantity of material is available, which poses the problem of developing a suitable experimental tool to reduce material consumption. Using microfluidic systems to form microdroplets, as increasingly done over the past decade,[3] could provide the solution, allowing the manipulation of fluids on submillimeter scale.[4,5] Our microfluidic system dedicated to crystallization is based on the generation of nanocrystallizers (nL droplets) isolated from each other and in which crystallization can occur independently.[6] Moreover we are able to form hundreds of droplets, which are monodispersed in size and in chemical composition, without using surfactant. Hence we can generate a large number of experiments per condition for statistical studies, in order to deal with the stochasticity of the phenomenon of nucleation, while consuming only small quantities of material.

Transforming microfluidics into a versatile tool for the screening of crystallization conditions and phases offers promise for many potential applications.[7] Our goal is to create a microfluidic device compatible with all solvents and molecules. This device should be simple and easily incorporated into any laboratory, even those not specialized in microfluidics. Thus, we initially constructed a microfluidic system based on a T-shaped junction[8−10] coupled with Teflon tubing, which is resistant to many solvents,[11] rendering the device applicable to mineral,[12] organic[11] and biological materials.

Here, after studying the hydrodynamic properties of the system, we obtain control of droplet generation regimes by adjusting flow rates. We present scaling laws for droplet size, depending on the capillary number. We test the microfluidic setup with organic and mineral molecules, organic solvents and viscous media. Finally, replacing the T-junction with a cross-junction, we present crystallization experiments in which experimental conditions are varied by a precise control of input flows of solute and crystallization medium.

RESULTS AND DISCUSSION

Microfluidic setup. PEEK (polyether ether ketone) devices based on HPLC techniques; T-shaped (Figure 1a and b), as described previously,[9,11] or cross-shaped (Figure 1c and d) ("plug-factory") designs were used to form the droplets without addition of surfactants. Teflon tubing ("storage chip") was used because it is compatible with almost all organic solvents. Water, ethanol (Figure 3), acetone, ethyl acetate, acetonitrile, nitrobenzene and acetate were previously tested.[11,12] Moreover, no evaporation was observed after 1 week at room temperature. To ensure maximum versatility, we used Fluorinated oil FC-70 (Hampton research) for organic solvents and FMS oil (Hampton Research) for aqueous solvents. These oils show no or very low miscibility with corresponding solvents and good wettability with Teflon. The pending drop method was used to measure the interfacial energy between immiscible phases; method and setup were previously described.[13]

Crystallization solutions and oil were separately loaded using separate syringes placed in a temperature-controlled incubator (from room temperature to 65 °C). The homemade setup is presented in Figure 2 (available commercially - ANACRISMAT). The channel was filled with different batches of monoconcentrated droplets. A T-junction was used for hydrodynamics studies and a cross-junction for crystallization studies. With a T- junction, droplets of crystallizing solution can be dispersed in oil, supersaturation being generated by temperature variation. In a cross-junction, the supersaturation is directly created by mixing 2 solutions and simultaneously dispersing this solution in oil. The droplet concentration and composition were varied using a programmable multichannel syringe pump (neMESYS) and controlling the relative flow rates of the different solutions (solution 1 and solution 2 in Figure 2b—from several μL/h up to thousands of μL/h). Droplet sizes were controlled both via the channel size of the plug-factory and via the flow rates. The tubing containing the droplets was placed in a thermostated tubing-holder and

Received: January 23, 2015

DOI: 10.1021/acs.oprd.5b00122
Org. Process Res. Dev. XXXX, XXX, XXX−XXX

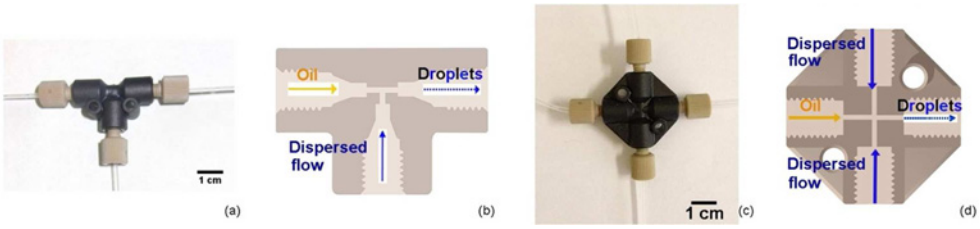

Figure 1. Photos and schemes of PEEK plug-factory junctions. (a) and (b) T-shaped; (c) and (d) cross-shaped. Schemes of PEEK Tee and Cross from IDEX Health and Science catalog.

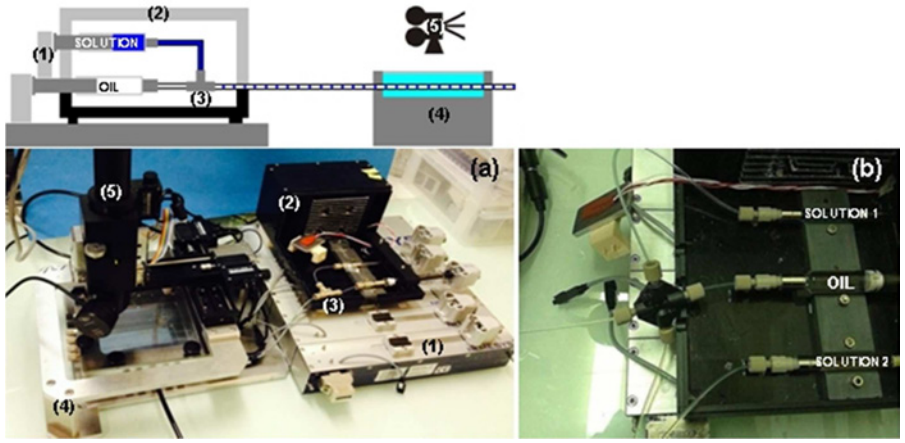

Figure 2. (a) Scheme and photograph of the homemade microfluidic setup: (1) syringe pump, (2) temperature controlled incubator, (3) T-junction, (4) thermostated tubing-holder (tubes are immersed in water for thermostating and observation), and (5) XYZ-motorized camera. (b) Cross-junction.

incubated (Figure 2a(4)), to obtain crystallization. Droplets were observed using an XYZ-motorized camera (OPTO) with variable zoom.

Droplet formation and volume with the T-junction. The dispersed phase (crystallization solution) is injected perpendicularly to the continuous phase (oil). Figure 3 shows

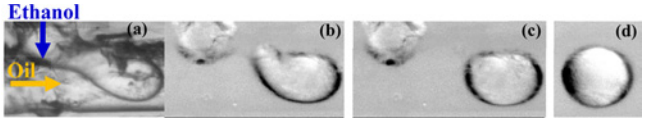

Figure 3. Microphotographs of ethanol droplets generated and transported by the flow of FC70 oil in a transparent T-junction (ETFE) of 508 μm of internal diameter: the capillary number *Ca* is 0.016, the ratio u_D/u_C between the dispersed phase (ethanol) and the continuous phase (oil) velocities is 0.1, and the total flow velocity u_{TOT} (u_D + u_C) is 5.1 m/s. Background was removed from images (b–d) using ImageJ software (NIH).

ethanol plugs generated and transported by the flow of oil in a transparent T-junction (ETFE); observations were made under an optical microscope (Zeiss Axio Observer D1) equipped with a camera sCMOS (Neo, ANDOR Technology). The channel diameters were 508 μm (P-729 IDEX). Droplets were spontaneously formed and transported when the flow of crystallization medium was sheared into the continuous flow of oil (Figure 3), leading to a dispersed phase of crystallization medium. A complete description of the different regimes of droplet formation is beyond the scope of this paper. The resulting droplets of the dispersed phase are monodispersed in size and uniformly spaced (Figure 4).

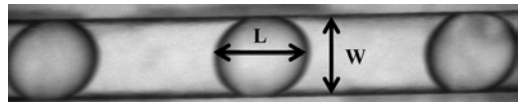

Figure 4. Photo of ethanol droplets surrounded by FC70 oil equally sized and uniformly spaced, in Teflon tubing of 508 μm internal diameter.

The scaling law of droplet formation by cross-flow shear method in T-junction microfluidic devices has been systematically studied, and it was observed that droplet formation is controlled by a competition between the interfacial energy and the viscous or shear force imposed by the continuous phase.[8,10,16−19] The relative strength of the two is expressed by the capillary number *Ca* defined as

$$Ca = \frac{\mu_c \times u_c}{\gamma} \quad (1)$$

where u_c is the continuous phase velocity calculated with the ratio between the flow rate of the continuous phase and the section of the channel, μ_c is the continuous phase viscosity (Table 1), and γ is the interfacial energy between the continuous and the dispersed phases (Table 2). *Ca* values characterizing the flow of the continuous phase in the channel are shown in Table 3. A low *Ca* indicates that the interfacial energy is strong compared to viscous stresses and dominates the shear force. Hence droplets tend to minimize their surface area. We characterized the droplet size using a normalized size given by the droplet length/width ratio (L/W). We measured L and calculated L/W for our experimental conditions, $0.002 \leq Ca \leq 0.12$ (Figure 4 and Table 3). The results are shown in Figure 5. This droplet formation regime is the dripping regime

DOI: 10.1021/acs.oprd.5b00122
Org. Process Res. Dev. XXXX, XXX, XXX−XXX

Table 1. Physical Properties of the Phases

	FC70	FMS	Ethanol	PEG 8K 0%	PEG 8K 2.5%	PEG 8K 5%	PEG 8K 7.5%	PEG 8K 10%
Density ρ (kg/m^3)	1940	1250−1270	789	1003	1005	1006	1020	1027
Kinematic viscosity $\nu \times 10^6$ (m^2/s)	12	350−450	1.52	1.00	2.24[a]	2.75[b]	4.89[a]	8.70
Dynamic viscosity μ_c (10^{-2} × kg/(m × s))	2.33	43.75−57.15	0.12	0.10	0.23	0.28	0.50	0.89[c]

[a]Marcq personal communication. [b]Reference 14. [c]Reference 15 and percentage of PEG 8K in buffer solution.

Table 2. Interfacial Energy between Continuous and Dispersed Phases at 23°C

Interface	γ (mN/m)
Water/air	72.8
FC70/ethanol	6.7 (±3.75%)
FMS/PEG 0%	32.5 (±2.39%)
FMS/PEG 2.5%	21.5 (±3.57%)
FMS/PEG 5%	21.1 (±2.7%)
FMS/PEG 7.5%	20.9 (±4.31%)
FMS/PEG 10%	20.0 (±3.51%)

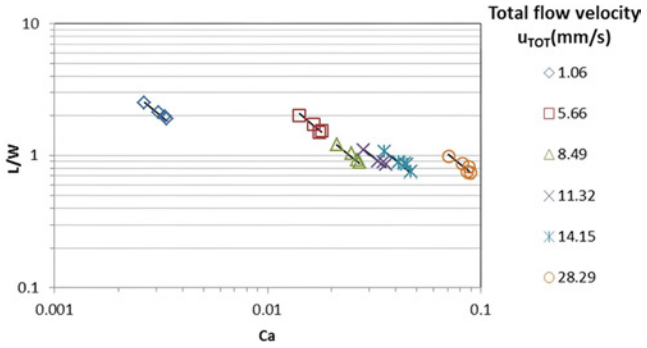

Figure 5. Evolution of L/W ratio versus *Ca* for different total flow velocities (mm/s) in a channel of 508 μm diameter (W). Lines represent data fitting with a $Ca^{-4/3}$ law.

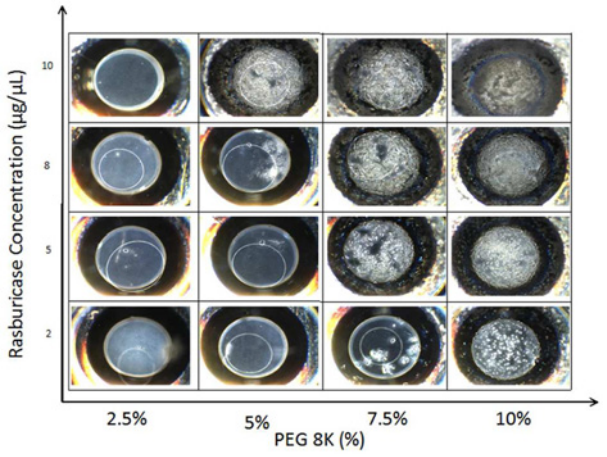

Figure 6. Rasburicase morphodrome in 10 μL microbatch (protein concentration vs PEG concentration).

that Xu et al.[18] obtained with $0.002 \leq Ca \leq 0.3$. Our values of L/W measured for different total flow velocities u_{TOT} (sum of ethanol and FC70 oil flow velocities) lead to a scaling law that depends on *Ca* and channel diameter (Figure 5): L/W scales with $Ca^{-4/3}$. Therefore, depending on absolute values of u_D (implied in u_{TOT}) and u_c (implied in *Ca* and u_{TOT}), droplet length L can be smaller than (L/W < 1), similar to (1 < L/W < 2) or much larger than (L/W > 2) the channel width W. In the case of L/W < 1, droplets are mobile in the continuous phase even when the channel is closed. Therefore, they can coalesce. When L/W > 2, droplets are called plugs.

Crystallization. To test our setup, we crystallized a biological macromolecule, rasburicase, in a viscous medium (see viscosities in Table 1). First, the microbatch method[20] was used for rapid screening of rasburicase crystallization conditions to determine the microfluidic experimental conditions. The conditions for this preliminary screening come from the work of Giffard et al.[21] Droplets were prepared by mixing the concentrated protein solution with the agent of crystallization or precipitant agent (PEG 8000 40%) in a 72-well microbatch plate (Hampton Research). Results are presented in Figure 6.

Since precipitation is observed as soon as the solutions are mixed for high concentrations of rasburicase (>8 μg/μL) and high percentages of PEG (>7.5%), it is obviously essential to mix the protein and PEG solution and form droplets at the same time. This is a potential problem with microfluidic methods because precipitates tend to adhere to the walls of the channels and perturb or even obstruct the flow, with the consequent risk of clogging the channel, one of the major drawbacks in microfluidics.[22,23] Another problem with microfluidic methods is the effect of the change of scale on nucleation kinetics: the smaller the volume the longer the induction time, all things being equal. Thus, the "scale-down" requires generation of higher supersaturation in the nanocrystallizers, with a risk of unwanted nucleation inside the syringe before droplet generation.

To avoid clogging and ensure higher supersaturation, we use a cross-shaped junction (Figure 2b) where the three fluids meet and mix at the intersection and generate droplets of reproducible composition (tested by off-line optical density measurement). The operating parameters ($0.0057 \leq u_c \leq 0.8587$ mm/s) were chosen so as to obtain $1 \leq L/W \leq 2$,

Table 3. *Ca* for Experimental Conditions of This Work (Channel Diameter of 508 μm)

Oil	Dispersed phase	Flow rate of the continuous phase (oil) (μL/h)	u_c (10^{-3} × (m/s))	μ_c (10^{-2} × kg/(m × s))	γ (mN/m)	*Ca* ($\times 10^{-2}$)
FC70	Ethanol	400	0.57	2.33	6.7	0.20
FC70	Ethanol	4000	5.66	2.33	6.7	1.97
FMS	PEG 0%	400	0.57	43.75	32.5	0.76
FMS	PEG 0%	4000	5.66	43.75	32.5	7.63
FMS	PEG 10%	400	0.57	43.75	20.0	1.24
FMS	PEG 10%	4000	5.66	43.75	20.0	12.40

DOI: 10.1021/acs.oprd.5b00122
Org. Process Res. Dev. XXXX, XXX, XXX−XXX

ensuring droplet homogeneity, for the following reasons. First, for long plugs of L/W > 2 there is a risk of a concentration gradient inside the plug after nucleation because mass transfer occurs solely via diffusion. Second, when droplets are generated, shearing interactions between the two dispersed phases and the continuous phase causes the mixing of the PEG and protein solutions inside the droplet, which Tice et al.[24] demonstrate works better with shorter plugs.

Droplets are generated at room temperature and stored at 5 and 20 °C. For high supersaturated conditions (10% PEG 8K and 10 μg/μL rasburicase), precipitates appear at the moment of droplet formation, leading to crystals by the Ostwald ripening mechanism (Figure 7a).[25] We focused on experimental conditions where no precipitates appear, but which permit nucleation after a few hours. For instance, at a lower supersaturation (7.5% PEG 8K and 2 μg/μL rasburicase), transparent drops form without precipitates, leading to a single crystal (Figure 7b). Figure 8 shows crystals obtained under different conditions, and Table 4 gives the representative statistical distribution of the number of crystals per droplet versus temperature for different protein concentrations. Only some of the 100−200 droplets per experimental condition are shown in Figure 8. Here the same conditions obviously produce different crystal habits and phases (the crystallization of a protein gives rise not to real polymorphs but to different crystalline phases of the same protein, because the different phases of the same protein have different compositions). It was previously shown in our laboratory that the different crystal habits of rasburicase correspond to two different phases.[26]

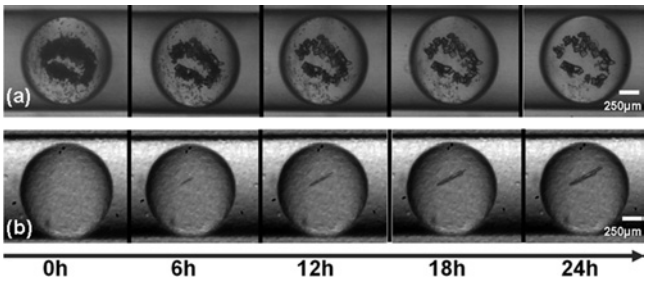

Figure 7. Time sequence of droplets for 24 h storage. (a) 10% PEG, 10 μg/μL rasburicase, at 20 °C. (b) 7.5% PEG, 2 μg/μL rasburicase, at 20 °C. See also Supporting Information videos.

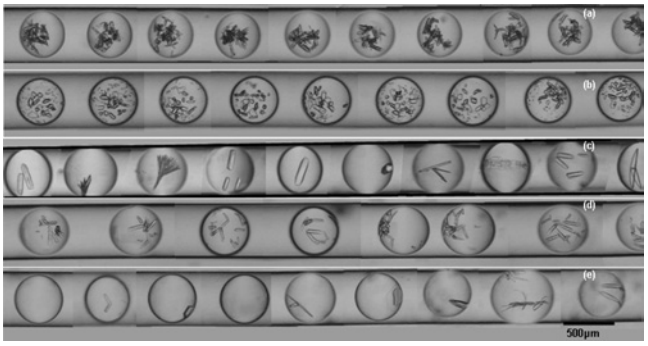

Figure 8. Photos of crystals obtained in 65 nL droplets after 24 h. (a) 10% PEG, 10 μg/μL rasburicase, at 5 °C. (b) 10% PEG, 10 μg/μL rasburicase, at 20 °C. (c) 5% PEG, 10 μg/μL rasburicase, at 5 °C. (d) 7.5% PEG, 5 μg/μL rasburicase, at 5 °C. (e) 7.5% de PEG, 5 μg/μL rasburicase, at 20 °C.

Table 4. Statistical Distribution of the Number of Crystals per Droplet versus Temperature for Different Protein Concentrations

			temp (°C)	
Rasburicase conc (mg/mL)	PEG conc (%)	[a]	5	20
10	10	0	0	0
		1	0	0
		>1	100	100
		N	107	109
10	5	0	6.1	51.1
		1	51.1	15.6
		>1	42. 8	33.3
		N	229	90[b]
5	7.5	0	0	30.2
		1	0	20.7
		>1	100	49.1
		N	146	159

[a]0, 1 and >1 correspond to 0, 1 and more than 1 crystals per droplet in percentage and N the total number of droplets. [b]experiment in 100 nL plugs (Figure.S1).

These results, with the highly dispersed number and phases of crystals presented in Figure 8 and Table 4, highlight the importance of carrying out statistical studies through a large number of experiments per condition because of the stochasticity of nucleation. Statistically, each crystallization condition should be tested from 50 to 100 times in order to order to obtain a good confidence level and thus to decide whether the result (crystallization success rate) is positive or negative. This is the main problem with the conventional crystallization assay robots, where typically a few hundred different conditions are tested only 1 to 5 times each, leading often to false negative results or nonreproducible positive results.

CONCLUSION

In this communication we present a simple and easy-to-use microfluidic setup for the crystallization of mineral, organic, and biological materials. The hydrodynamic properties of the setup are briefly presented, and then we test and validate this setup with viscous media by crystallizing a protein in an aqueous solution of PEG. We obtain nucleation data in nanocrystallizers of 65 and 100 nL. This study illustrates the importance of carrying out a large number of experiments per condition for statistical studies. Here, conditions are varied by a precise control of input flows of solute and crystallization medium. Future perspectives include screening crystallization conditions using this microfluidic setup.

EXPERIMENTAL SECTION

Testing molecules. The recombinant urate oxidase (Rasburicase) was supplied by Sanofi-Aventis without inhibitor in a phosphate buffer. The rasburicase was then purified by gel filtration chromatography on a Superdex S200PG system,[21] and concentrated by ultrafiltration on an Amicon cell to 20 μg/μL, in 0.05 M Tris buffer pH 7.5 containing 30 mM KCl. Series of PEG 8000 solution were prepared and used as agents of crystallization with concentrations in the range 2.5−10% w/v. Physical properties of the different phases are given in Table 1.

DOI: 10.1021/acs.oprd.5b00122
Org. Process Res. Dev. XXXX, XXX, XXX−XXX

■ ASSOCIATED CONTENT

Supporting Information

Experiment in 100 nL plugs, and videos of Figure 7a (Ostwald ripening) and Figure 7b (Nucleation and growth) (AVI). The Supporting Information is available free of charge on the ACS Publications website at DOI: 10.1021/acs.oprd.5b00122.

■ AUTHOR INFORMATION

Corresponding Author

*Phone: 336 6292 2866. Fax: 334 9141 8916. E-mail: veesler@cinam.univ-mrs.fr.

Notes

The authors declare no competing financial interest.

■ ACKNOWLEDGMENTS

We thank Marjorie Sweetko for English revision. We thank Région PACA and C'Nano PACA for financial support. We thank Dr. M. El-Hajji (Sanofi) for the rasburicase and Minh Phat La, B. Benhaim, T. Bactivelane (CINaM), and Mr. Audiffren (ANACRISMAT) for technical assistance.

■ REFERENCES

(1) Stevens, R. C. *Curr. Opin. Struct. Biol.* **2000**, *10*, 558−563.
(2) Morissette, S. L.; Soukasene, S.; Levinson, D.; Cima, M. J.; Almarsson, O. *Proc. Natl. Acad. Sci. U.S.A.* **2003**, *100*, 2180−2184.
(3) Leng, J.; Salmon, J. B. *Lab Chip* **2009**, *9*, 24−34.
(4) Squires, T. M.; Quake, S. R. *Rev. Mod. Phys.* **2005**, *77*, 977.
(5) Lorber, N.; Sarrazin, F.; Guillot, P.; Panizza, P.; Colin, A.; Pavageau, B.; Hany, C.; Maestro, P.; Marre, S.; Delclos, T.; Aymonier, C.; Subra, P.; Prat, L.; Gourdon, C.; Mignard, E. *Lab Chip* **2011**, *11*, 779−787.
(6) Laval, P.; Salmon, J.-B.; Joanicot, M. *J. Cryst. Growth* **2007**, *303*, 622−628.
(7) Li, L.; Ismagilov, R. F. *Annu. Rev. Biophys.* **2010**, *39*, 139−158.
(8) Thorsen, T.; Roberts, R. W.; Arnold, F. H.; Quake, S. R. *Phys. Rev. Lett.* **2001**, *86*, 4163−4166.
(9) Dombrowski, R. D.; Litster, J. D.; Wagner, N. J.; He, Y. *Chem. Eng. Sci.* **2007**, *62*, 4802−4810.
(10) Nisisako, T.; Torii, T.; Higuchi, T. *Lab Chip* **2002**, *2*, 24−26.
(11) Ildefonso, M.; Candoni, N.; Veesler, S. *Org. Process Res. Dev.* **2012**, *16*, 556−560.
(12) Rodríguez-Ruiz, I.; Veesler, S.; Gómez-Morales, J.; Delgado-López, J. M.; Grauby, O.; Hammadi, Z.; Candoni, N.; García-Ruiz, J. M. *Cryst. Growth Des.* **2014**, *14*, 792−802.
(13) Bukiet, F.; Couderc, G.; Camps, J.; Tassery, H.; Cuisinier, F.; About, I.; Charrier, A.; Candoni, N. *J. Endodontics* **2012**, *38*, 1525−1529.
(14) Ninni, L.; Burd, H.; Fung, W. H.; Meirelles, A. J. A. *J. Chem. Eng. Data* **2003**, *48*, 324−329.
(15) Gonzalez-Tello, P.; Camacho, F.; Blazquez, G. J. *Chem. Eng. Data* **1994**, *39*, 611−614.
(16) Cristini, V.; Tan, Y.-C. *Lab Chip* **2004**, *4*, 257−264.
(17) Garstecki, P.; Fuerstman, M. J.; Stone, H. A.; Whitesides, G. M. *Lab Chip* **2006**, *6*, 437−446.
(18) Xu, J. H.; Li, S. W.; Tan, J.; Luo, G. S. *Microfluid Nanofluid* **2008**, *5*, 711−717.
(19) Baroud, C. N.; Gallaire, F.; Dangla, R. *Lab Chip* **2010**, *10*, 2032−2045.
(20) Ducruix, A.; Giégé, R. *Crystallization of Nucleic Acids and Proteins A Practical Approach*, 2nd ed.; Oxford University Press: Oxford, 1999; p 460.
(21) Giffard, M.; Colloc'h, N.; Ferté, N.; Castro, B.; Bonneté, F. *Cryst. Growth Des.* **2008**, *8*, 4220−4226.
(22) Poe, S. L.; Cummings, M. A.; Haaf, M. P.; McQuade, D. T. *Angew. Chem., Int. Ed.* **2006**, *45*, 1544−1548.
(23) Zheng, B.; Roach, L. S.; Ismagilov, R. F. *J. Am. Chem. Soc.* **2003**, *125*, 11170−11171.
(24) Tice, J. D.; Song, H.; Lyon, A. D.; Ismagilov, R. F. *Langmuir* **2003**, *19*, 9127−9133.
(25) Candoni, N.; Grossier, R.; Hammadi, Z.; Morin, R.; Veesler, S. *Protein Pept. Lett.* **2012**, *19*, 714−724.
(26) Vivares, D.; Veesler, S.; Astier, J. P.; Bonneté, F. *Cryst. Growth Des.* **2006**, *6*, 287−292.

DOI: 10.1021/acs.oprd.5b00122
Org. Process Res. Dev. XXXX, XXX, XXX−XXX